J Mol Model (2008) 14:29–37
DOI 10.1007/s00894-007-0247-y

ORIGINAL PAPER

G2, G3, and complete basis set calculations on the thermodynamic properties of triazane

Ryan M. Richard · David W. Ball

Received: 8 June 2007 / Accepted: 26 September 2007 / Published online: 26 October 2007

Abstract As a follow-up study to our study on tetrazane (N_4H_6), we present computed thermodynamic properties of triazane (N_3H_5). Calculated properties include optimized geometries, infrared vibrations, enthalpy of formation, enthalpy of combustion, and proton affinities. We have also mapped the potential energy surface as the molecule is rotated about the N-N bond. We have predicted a specific enthalpy of combustion for triazane of about -20 kJ g^{-1}.

Keywords G2 · G3 · CBS-QB3 · CBS-APNO · High energy materials · Thermodynamic properties · Triazane

Introduction

Research involving the search for and synthesis of new high energy (HE) materials is an ongoing quest. There are many molecules that fall into this category, and analysis of their characteristics yields several trends in structure and chemistry. These trends include strained ring structures, molecules that are unstable with respect to their combustion products, and the inclusion of various nitrogen containing functional groups, such as nitro, nitrato, and amine groups [1]. Other studies offer additional traits, such as using boron and aluminum due to the stability of their combustion products [2]. Previously, Ball [3] studied the thermodynamic properties of tetrazane, the nitrogenous analog of butane; he calculated an enthalpy of formation of about 293 kJ mol^{-1} for tetrazane. As a follow-up to this study, here we characterize the nitrogenous analog of propane, triazane.

Triazane can exist in several conformations.

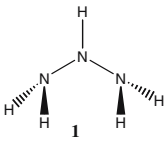

1

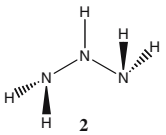

2

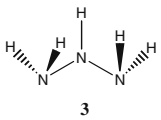

3

Very little previous work has been done on triazane; one of the earliest studies that makes mention of triazane was done by Schmitz et al. [4]. They were studying the formation of diimides by amination reactions. They claimed that the presence of NH_3 in the overall reaction was explainable by the decomposition of triazane, which they proposed was created from the hydrazine involved in the reaction. However, they offer no additional evidence to support this claim. Kim et al. [5] successfully synthesized both triazane and cyclotriazane using ammonia gas, sodium zeolite, and silver metal. Using crystallographic analysis, they verified the presence of these compounds and determined several structural parameters. Schlegel and Skancke [6] computed the thermodynamic properties of several nitrogen containing molecules using the G2 method, a HF/6-31G*// HF/6-31G* calculation, and a MP2/6-31G*// MP2/6-31G* with a frozen core calculation. They reported optimized structural parameters, infrared vibrational frequencies, and enthalpies of formation. Most recently Fujii et al. [7] studied the hydronitrogen species that were created by microwave discharge of hydrazine using lithium cation attachment mass spectrometry. They noted a peak in their spectra having a mass to charge ratio equal to that expected of triazane and speculated as to the reactions that may have caused it.

R. M. Richard · D. W. Ball (✉)
Department of Chemistry, Cleveland State University,
2121 Euclid Avenue,
Cleveland, OH 44115, USA
e-mail: d.ball@csuohio.edu

Computational details

All calculations were performed on a personal computer using either the Gaussian 98 [8] program or the Gaussian 03 [9] computational chemistry program. Structures and vibrations were viewed using GaussView 2.1 [10] and GaussView 3.09 [11]. Computational methods used were the G2 [12], G3 [13], and two complete basis set (CBS) [14] methods. The infrared spectra were generated using the SWizard program [15] using a Lorentzian lineshape with a 15 cm^{-1} bandwidth at half height. The enthalpy of formation was calculated using the reverse atomization reaction, reaction 1, which is the same for each conformation of triazane.

$$3N(g) + 5H(g) \rightarrow N_3H_5(g) \quad (1)$$

This reaction was corrected for the gaseous formation of the reactants using data from the NIST website [16]. Using the enthalpy of formation calculated from reaction 1, we were then able to calculate the enthalpy of combustion for triazane using reaction 2.

$$N_3H_5(g) + 5/2O_2(g) \rightarrow 3/2N_2(g) + 5/2H_2O(\ell) \quad (2)$$

Dividing reaction 2 by the molar mass of triazane gives the specific enthalpy of combustion.

The proton affinity (PA) of a molecule is a measure of the molecule's Lewis base strength. The proton affinity is the negative of the change in enthalpy of the protonation reaction; for triazane this reaction is given in reaction 3.

$$N_3H_5(g) + H^+ \rightarrow N_3H_6^+(g)\, PA \equiv -\Delta H_{rxn} \quad (3)$$

For this reaction, we assumed that a nitrogen atom is the site of protonation in the molecule. It should be noted that triazane has two chemically different nitrogen atoms and so the proton affinity must be calculated for each of these two sites.

Results and discussions

Optimized geometries

Tables 1, 2, 3 give the optimized parameters for triazane for conformations 1–3. Figures 1, 2, and 3 show the optimized geometry for each of the conformations. A subscript "t" in any of the tables refers to the terminal nitrogen atom of the molecule. Experimental data is included in the tables where it is available. It should be noted that the experimentally obtained data did not differentiate between the three distinct conformations and so it is included for all three conformations.

Table 1 lists the optimized parameters for conformation 1 (structure **1**). The data in Table 1 is consistent among the different calculational methods, with the largest variation in bond length being 0.003 Å and the largest variation in bond angle being 0.9° for the dihedral angle. Comparing the calculated parameters to those experimentally determined by Kim et al. [5], there is quite a discrepancy; Kim et al. determined a N_t-N bond length of 1.6 Å, whereas we calculated the N_t-N bond length to be about 1.425 Å. This is a discrepancy of 0.175 Å. A similar discrepancy exists for the N_tNN_t angle, Kim et al. [5] determined a N_tNN_t angle of 107°, while we calculated the same angle to be about 116°, a difference of 9°. The reason for these discrepancies stems from the conditions under which the measurements were conducted. Kim et al. [5] carried out their experiment using Ag^+-exchanged zeolite; this means that the triazane was not measured in the gas phase as an isolated compound as we simulated in our calculations, but in the presence of a cation, Ag^+. Due to the strong Lewis-base like characteristics of triazane (see proton affinity discussion), one would expect it to donate its electrons readily, and indeed it does. Based on the crystallography study by Kim et al. [5] the triazane molecules actually form the complex $Ag_2(N_3H_5)_3^{2+}$, where each silver atom is still part of the silver exchanged zeolite. This means that three triazane molecules are surrounded by two silver atoms; the silver atoms are flanking the triazane molecules, causing the terminal nitrogen atoms of each triazane molecule to be

Table 1 Optimized geometric parameters for conformation 1 (all bond lengths are in Å, and all angles in degrees)

Parameter	G2, G3	CBS-QB3	CBS-APNO	Experimental [5]
r (N_t-N)	1.427	1.424	1.424	1.6
r (N_t-H)	1.010	1.010	1.010	
r (N-H)	1.010	1.010	1.010	
α (N_tNN_t)	116.1	117.1	115.9	107
α (HN_tH)	106.9	107.6	106.7	
α (N_tNH)	106.0	106.7	106.0	
δ (N_tNN_t-H)	79.8	80.0	78.9	

Table 2 Optimized geometric parameters for conformation 2 (all bond lengths are in Å, and all angles in degrees)

Parameter	G2, G3	CBS-QB3	CBS-APNO	Experimental [5]
r (N_t-N)	1.426	1.422	1.423	1.6
r (N_t-H)	1.020	1.020	1.020	
r (N-H)	1.010	1.010	1.010	
α (N_tNN_t)	111.4	112.8	111.7	107
α (HN_tH)	105.4	106.2	105.5	
α (N_tNH)	104.9	105.8	105.1	
δ (N_tNN_t-H)	96.7	97.3	96.4	

Table 3 Optimized geometric parameters for conformation 3 (all bond lengths are in Å, and all angles in degrees)

Parameter	G2, G3	CBS-QB3	CBS-APNO	Experimental [5]
r (N_t-N)	1.426	1.423	1.425	1.6
r (N_t-H)	1.020	1.010	1.010	
r (N-H)	1.020	1.010	1.010	
α (N_tNN_t)	109.2	110.8	109.5	107
α (HN_tH)	107.7	108.9	107.8	
α (N_tNH)	109.7	110.3	109.5	
δ (N_tNN_t-H)	92.4	94.5	92.3	

pulled toward them. This stretching of the triazane molecule results in the elongation of the N_t-N bond.

Comparing the data in Table 1 to the computationally obtained data by Schlegel and Skancke [6] shows good agreement, especially between their frozen core MP2 calculations and our four methods; their MP2 method calculates angles that are within about 1° of ours, and bonds that are within 0.01 Å. Schlegel and Skancke also performed calculations at the Hartree-Fock (HF) level of theory; the data obtained from these calculations did not match our data as well as the data calculated from the MP2 level of theory, but was still in good agreement. The largest discrepancies were 0.02 Å for the N_t-N bond, and about 1.5° for the HN_tH angle.

Table 2 lists the optimized parameters for conformation 2 (structure **2**) of triazane. The values in Table 2 are again consistent among the different methods, with maximum deviations of 0.003 Å for the N_t-N bond, and 1.1° for the N_tNN_t angle. Again the values in Table 2 do not agree well with the experimentally derived values; this is also attributed to the different environment under which the measurements were made. Between our four calculations and Schlegel's and Skancke's [6] MP2 calculation, all bonds agree within 0.01 Å, and all angles agree within 2°. Their HF calculation had the same discrepancy for the bond lengths of this conformation as it did for 1; however, the HF calculation now predicts angles that have a discrepancy of 8° compared to our predicted angles. Schlegel and Skancke calculated HN_tH angles of about 98°, where we calculated this angle to be about 106°.

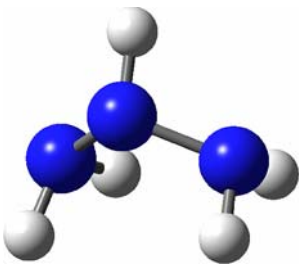

Fig. 1 Triazane in conformation **1**. See Table 1 for optimized parameters

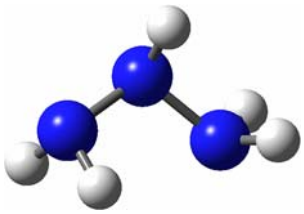

Fig. 2 Triazane in conformation **2**. See Table 2 for optimized parameters

Table 3 lists the optimized parameters for conformation 3 (structure **3**) of triazane. The predicted values in this table are again in good agreement among the four calculation methods. The largest bond difference is 0.01 Å, and the largest angle difference is 2.1°. Similar to the data in Tables 1 and 2, the values in Table 3 do not agree well with the experimentally measured values and again the silver cations' presence are presumed to be the cause. Comparing the data in Table 3 to the data obtained by Schlegel and Skancke [6] again yields good agreement between the MP2 calculation and our four calculations; again all bonds are within 0.01 Å and all angles are within 1°. The Hartree-Fock calculation is within the same degree of agreement as it was for Table 2.

Comparing the predicted data in Tables 1, 2, and 3 to the predicted data of tetrazane [3], it becomes apparent that there is much similarity. Tetrazane has three N-N bonds, two of which contain a terminal nitrogen atom; these bonds are of similar length to the N_t-N bonds found in triazane. Ball [3] predicts values of 1.411 Å and 1.437 Å for the cis and trans isomers of tetrazane respectively, triazane falls directly between these two values with a bond length of about 1.425 Å. Triazane's N-H bond is slightly longer than the N-H bonds found in either isomer of tetrazane, 1.010 Å for the N-H bond in triazane, 1.001 Å for the cis isomer, and 1.006 Å for the trans isomer Å. The N_t-H bonds in triazane are also longer than those found in tetrazane, 1.015 Å for triazane, 1.002 Å for the cis isomer, and 1.003 Å for the trans isomer of tetrazane. The N_tNN_t angle in triazane is larger than the N_tNN angles found in tetrazane, about 113° for triazane, 111.9° for the cis isomer, and 105.6° for the trans isomer of tetrazane.

Conformational energies

All four methods predict that conformation **1** is the lowest-energy conformation of triazane. Conformation **2** is next

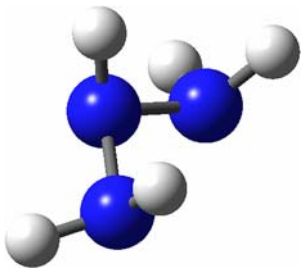

Fig. 3 Triazane in conformation **3**. See Table 3 for optimized parameters

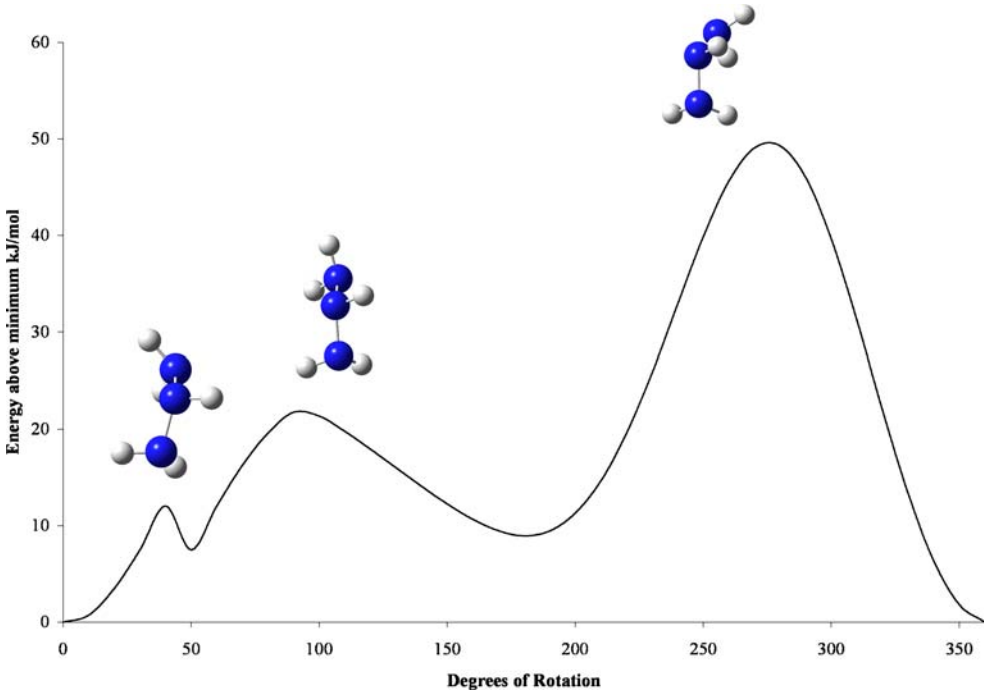

Fig. 4 PES of a rigid scan of rotation about the N_t-N bond in **1**

lowest, calculated as about 3.2–3.9 kJ mol^{-1} higher in energy than **1**. Conformation **3** is the highest-energy structure, having an energy 21.2–21.6 kJ mol^{-1} higher than conformation **1**, depending on method. That the increase in energy in going from **2** to **3** is several time larger than going from **1** to **2** suggests that steric hindrance in the molecule is not solely due to the central N-H moiety in the molecule.

Analogous to Ball's [3] study on tetrazane, we have calculated the potential energy surface (PES) for triazane's minimum energy conformation, 1, by rotation along the N_t-N bond at the HF level of theory using the 6-31G* basis

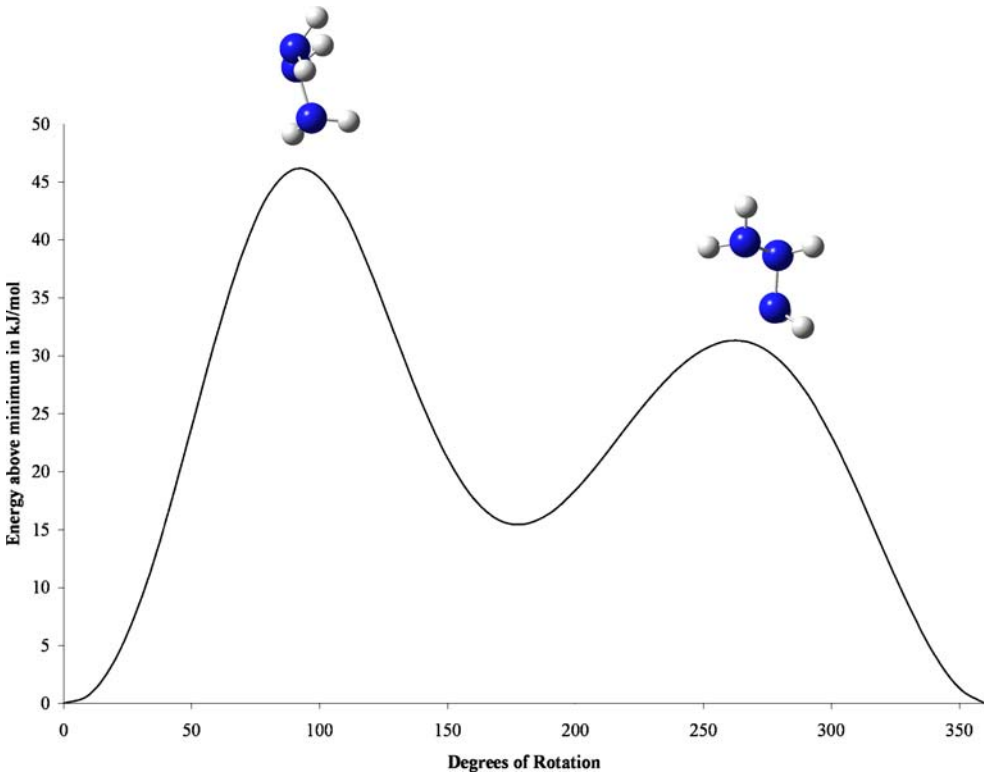

Fig. 5 PES for a rigid scan about the N_t-N bond in **2**

Table 4 Vibrational frequencies and intensities for conformation **1** of triazane (all vibrational frequencies are in cm^{-1}, and all intensities are km mol^{-1})

G2, G3	CBS-QB3	CBS-APNO	Description
361.7 (1.7)	343.8 (0.2)	354.7 (1.4)	asym N_tH_2 rock
476.8 (73.2)	459.9 (52.6)	473.0 (62.7)	sym N_tH_2 rock
539.0 (4.6)	485.2 (6.8)	533.9 (3.5)	N_tNN_t bend
925.9 (76.8)	788.7 (60.6)	922.7 (75.1)	N-H rock
1007.3 (328.1)	842.8 (305.3)	978.9 (302.9)	asym N_tH_2 wag
1072.7 (33.8)	976.0 (28.7)	1051.2 (28.3)	sym N_tH_2 wag
1263.6 (0.2)	1096.1 (5.5)	1260.3 (1.5)	asym N-N_t stretch
1301.1 (43.1)	1172.8 (28.0)	1276.5 (40.2)	sym N_tH_2 wag
1374.7 (2.6)	1247.6 (4.3)	1361.7 (2.1)	asym N_tH_2 twist
1496.7 (15.3)	1362.9 (11.9)	1482.7 (14.8)	sym N_tH_2 twist
1677.1 (<0.1)	1519.4 (<0.1)	1665.4 (<0.1)	N-H wag
1850.6 (1.5)	1674.5 (3.3)	1821.0 (0.6)	asym N_tH_2 bend
1875.8 (36.3)	1699.7 (31.7)	1843.0 (38.4)	sym N_tH_2 bend
3660.5 (15.8)	3362.5 (42.8)	3656.3 (13.4)	sym N_t-H stretch
3668.6 (6.1)	3376.2 (6.6)	3664.5 (3.3)	asym N_t-H stretch
3796.3 (1.2)	3521.6 (1.5)	3780.8 (0.3)	sym N_tH_2 stretch
3806.7 (<0.1)	3536.1 (<0.1)	3792.0 (<0.1)	asym N_tH_2 stretch
3832.2 (34.6)	3554.9 (2.1)	3815.2 (6.8)	N-H stretch

set. Figure 4 shows the PES for **1**; **2** is found along **1**'s PES and corresponds to the relative minimum at 180° of rotation. The PES shows two relative energy maximums along with the absolute energy maximum. The structures for all three maxima are superimposed on Fig. 4. At about 50 kJ per mole more energy than **1**, the absolute maximum occurs; this structure corresponds to two of the three lone pairs of electrons being eclipsed. Based on Fig. 4, the maximum energy barrier for rotation about the N_t-N bond is about 50 kJ mol^{-1}.

Figure 5 shows the PES for **2**, also using a HF/6-31G* calculation; **3** appears as the relative minimum around 180 degrees of rotation. Figure 5 has two maxima and the structures for the maxima are superimposed on the PES. The absolute maximum on this figure also corresponds to two of the three lone pairs eclipsed. Based on Fig. 5, the maximum energy barrier for rotation about the N_t-N bond is about 47 kJ mol^{-1}.

Compared to tetrazane, **1**'s energy barrier is much lower, about 50 kJ mol^{-1} compared to 80 and 95 kJ mol^{-1} for the cis and trans isomers of tetrazane [3]. Conformer **2**'s energy barrier is much higher due to steric hindrance between the unmoving N_tH_2 group and the NH group that is not present in **1**'s maximum.

Table 5 Vibrational frequencies and intensities for conformation **2** of triazane (all vibrational frequencies are in cm^{-1}, and all intensities are km mol^{-1})

G2, G3	CBS-QB3	CBS-APNO	Description
280.3 (86.8)	233.4 (68.4)	274.0 (75.3)	sym N_tH_2 rock
388.4 (14.7)	371.8 (8.9)	390.4 (13.4)	asym N_tH_2 rock
544.4 (34.6)	496.8 (36.1)	542.4 (34.4)	N_tNN_t bend
923.3 (28.9)	755.9 (28.5)	911.8 (28.8)	N-H rock
1031.4 (152.7)	857.0 (147.0)	1008.1 (152.4)	sym N_tH_2 wag
1115.7 (116.9)	999.5 (104.4)	1085.9 (105.5)	asym N_tH_2 wag
1226.2 (47.6)	1076.0 (21.6)	1210.0 (45.5)	N-N_t stretch
1332.1 (35.5)	1198.5 (33.2)	1313.0 (23.5)	N-N_t stretch
1407.9 (7.4)	1264.3 (3.7)	1393.1 (4.6)	sym N_tH_2 twist
1493.6 (8.6)	1348.9 (6.3)	1475.0 (9.3)	asym N_tH_2 twist
1680.1 (2.2)	1514.3 (3.2)	1667.2 (3.0)	N-H wag
1850.4 (15.3)	1667.7 (11.4)	1817.5 (16.8)	N_tH_2 bend
1878.5 (18.2)	1701.3 (16.1)	1844.4 (18.2)	N_tH_2 bend
3685.3 (7.1)	3398.9 (15.3)	3678.5 (5.8)	sym N_t-H stretch
3697.4 (7.4)	3430.9 (14.5)	3691.0 (5.6)	sym N_t-H stretch
3768.2 (2.3)	3489.5 (1.8)	3757.3 (0.9)	N-H stretch
3805.6 (1.0)	3532.2 (<0.1)	3790.2 (1.5)	asym N_t-H stretch
3817.9 (2.0)	3549.3 (0.4)	3803.9 (2.7)	asym N_t-H stretch

Table 6 Vibrational frequencies and intensities for conformation **3** of triazane (all vibrational frequencies are in cm^{-1}, and all intensities are km mol^{-1})

G2, G3	CBS-QB3	CBS-APNO	Description
222.7 (13.8)	203.1 (15.1)	229.2 (12.6)	asym N_tH_2 rock
307.1 (77.9)	290.7 (59.8)	304.3 (67.8)	sym N_tH_2 rock
585.8 (24.6)	542.8 (24.3)	583.2 (26.0)	N_tNN_t bend
929.9 (52.3)	755.3 (57.2)	915.6 (64.4)	N-H rock
946.2 (16.7)	731.9 (26.0)	911.6 (9.8)	asym N_tH_2 wag
1083.6 (173.6)	952.5 (185.8)	1054.8 (178.9)	sym N_tH_2 wag
1196.1 (100.9)	1077.7 (29.9)	1179.3 (68.4)	N-H rock
1317.1 (3.1)	1171.8 (9.5)	1306.1 (6.3)	asym N_t-N stretch
1423.3 (0.7)	1283.6 (0.3)	1407.7 (0.2)	asym N_tH_2 twist
1487.1 (7.0)	1337.3 (4.3)	1468.6 (6.7)	sym N_tH_2 twist
1684.6 (7.0)	1505.2 (8.2)	1671.3 (9.0)	N-H wag
1842.6 (10.1)	1664.2 (8.8)	1811.4 (14.0)	asym N_tH_2 bend
1871.2 (12.2)	1689.3 (10.8)	1838.1 (11.5)	sym N_tH_2 bend
3684.2 (26.3)	3408.4 (24.0)	3683.3 (16.6)	sym N_t-H stretch
3703.9 (6.0)	3441.6 (17.1)	3699.7 (4.8)	asym N_t-H stretch
3713.5 (3.4)	3445.0 (9.8)	3710.5 (2.2)	sym N_tH_2 stretch
3824.5 (1.6)	3564.2 (0.2)	3812.4 (2.0)	asym N_t-H stretch
3824.7 (0.9)	3564.3 (0.8)	3812.7 (1.7)	sym N_t-H stretch

Vibrations and vibrational spectra

The predicted vibrational frequencies and intensities for each conformation of triazane are located in Tables 4, 5, and 6, where Table 4 corresponds to conformer **1**, etc. Figure 6 shows the predicted spectra of each conformation of triazane using the vibrational frequencies and intensities predicted by the G2 method. Conformers **1** and **3** have C_s symmetry, and **2** has C_1 symmetry. The vibrations transform as:

$$\Gamma(1 \text{ and } 3) = 10\,A' \oplus 8A'' \qquad \text{in } C_s$$

$$\Gamma(2) = 18\,A \qquad \text{in } C_1$$

Because both symmetry species are active in C_s symmetry and the A mode is active in C_1 symmetry, all three conformations should have 18 infrared active vibrations. All four calculation methods predict 18 infrared active vibrations; however, some of these vibrations absorb very weakly, so less than 18 absorptions may be visible in the vibrational spectra.

Comparing the data in Tables 4, 5, and 6, it is apparent that the GX calculations and the CBS-APNO calculations predict frequencies that are usually within 10 cm^{-1} of one another. The CBS-QB3 method predicts vibrational fre-

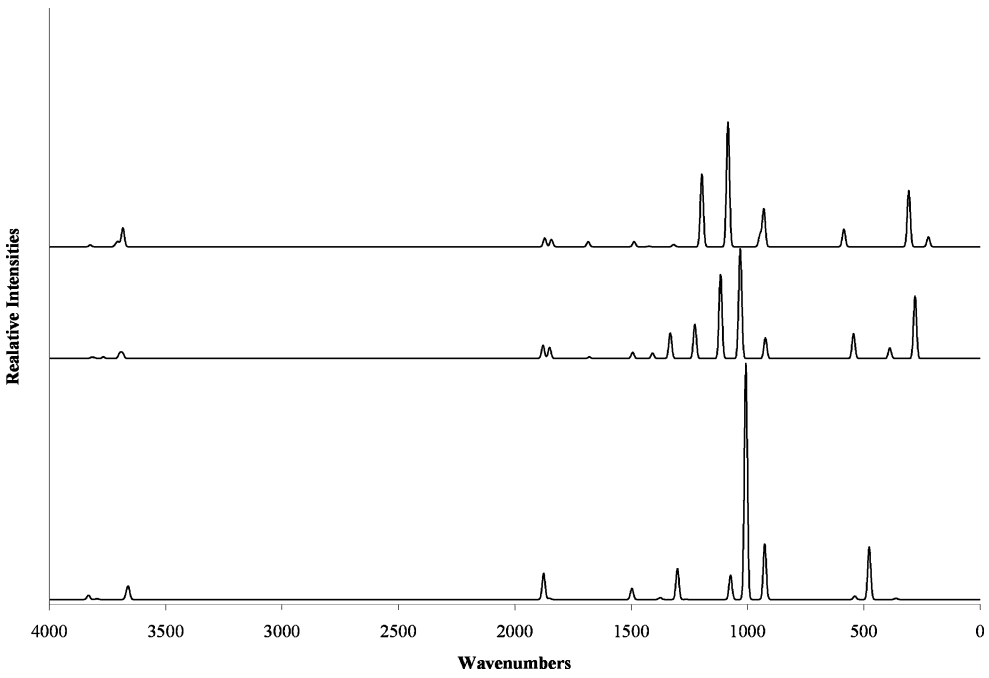

Fig. 6 Infrared spectra for the three conformations of triazane. All spectra are plotted to the same scale

Table 7 Enthalpies of formation for triazane, in kJ mol^{-1}

Conformation	G2	G3	CBS-QB3	CBS-APNO
1	195.7	204.1	196.5	199.2
2	199.5	207.8	199.9	203.0
3	216.8	225.6	217.9	220.5

quencies that are substantially lower than those predicted by the other three calculations, sometimes lower by 200 cm^{-1}. For 3 the two CBS methods predict that the N-H rock (755.3 cm^{-1}, 915.6 cm^{-1} for the CBS-QB3 and CBS-APNO respectively) and asym N_tH_2 wag (731.9 cm^{-1}, 911.6 cm^{-1} for the CBS-QB3 and CBS-APNO respectively) will switch relative energies relative to the GX method's predictions (See Table 6). Other than that switch, all four methods predict the same relative energies and descriptions for all vibrational frequencies.

Schlegel and Skancke [6] list frequencies and infrared intensities for conformations **2** and **3**, but not **1**. Comparing Table 5 to their predicted frequencies for **2** shows good agreement between their predicted values and those predicted by the CBS-QB3 method. Schlegel's and Skancke's calculated infrared intensities are in good agreement with those calculated by all four methods. Table 6 agrees with Schlegel's and Skancke's predicted values to the same extent as Table 5 did.

Figure 6 suggests that it would be hard to tell the difference between **2** and **3** due to their similarity; conformations **2** and **3**'s spectra differ by only a couple low intensity absorptions. Conformation **1**'s spectra shows significant difference compared to **2** and **3**'s spectra indicating that it should be possible to determine whether one has isolated conformation **1** or not.

Energies of reaction

Table 7 lists the enthalpies of formation for each conformation of triazane. The enthalpies of **1** and **2** are very similar, around -910 to -920 kJ mol^{-1}, indicating that rotation of one N_tH_2 group does not increase the energy very much, only about 3 kJ mol^{-1}; however, rotation of the second N_tH_2 group to yield conformation **3** does impart a significant energy gain of about 20 kJ mol^{-1}, bringing the enthalpy of combustion to about -930 to -940 kJ mol^{-1}.

Table 8 Enthalpies of combustion for triazane, in kJ mol^{-1}

Conformation	G2	G3	CBS-QB3	CBS-APNO
1	−910.2	−918.6	−911.2	−913.8
2	−914.1	−922.4	−914.4	−917.5
3	−931.4	−940.2	−932.5	−935.1

Table 9 Specific enthalpies of combustion for triazane, in kJ g^{-1}

Conformation	G2	G3	CBS-QB3	CBS-APNO
1	−19.3	−19.5	−19.4	−19.4
2	−19.4	−19.6	−19.4	−19.5
3	−19.8	−20.0	−19.8	−19.9

Schlegel and Skancke [6] calculated enthalpy of formation values for **2** at 0 K using two reactions, a formation reaction and an atomization reaction. For the formation reaction they predicted values of 283.7, 305.9, and 198.74 kJ mol^{-1} for a HF/6-31G*// HF/6-31G*, a MP2/6-31G*// MP2/6-31G*, and a G2 calculation, respectively. For the atomization reaction they obtained values of 1153.1, 449.4, 195.0 kJ mol^{-1} using the same methods. Our values are calculated at 298 K using an atomization reaction and should be slightly higher, which is seen in comparing our G2 value to Schlegel's and Skancke's [6] predicted G2 value. Schlegel and Skancke mention in their paper that the HF and MP2 levels of theory with a 6-31G* basis set are inadequate for determining the enthalpy of formation; this is in agreement with our study, as seen by their wide deviation from our predicted values.

Ball [3] calculated the enthalpy of formation of tetrazane using a reverse atomization reaction and obtained values of 292.0, 303.9, 292.6, and 298.7 kJ mol^{-1} for the G2, G3, CBS-QB3, and CBS-APNO calculations, respectively. These values are about 100 kJ mol^{-1} higher than those obtained for **1** and **2** here, and about 80 kJ mol^{-1} higher than those predicted for **3**. For further comparison, propane in the gas phase has an enthalpy of formation of -104.7 kJ mol^{-1} [16].

Table 8 lists the predicted enthalpies of combustion for the three conformations of triazane. The values show the same range of variance as the enthalpies of formation due to the nature of the calculation. The difference in combustion enthalpy is small among the three conformations, but becomes even less significant when comparing the specific enthalpies of combustion.

Table 9 lists the predicted specific enthalpies of combustion for each of the three conformations of triazane.

Table 10 Proton affinities for triazene, in kJ mol^{-1}

Conformation	G2	G3	CBS-QB3	CBS-APNO
1_t	873.1	874.5	872.7	874.8
1	863.0	864.3	861.8	864.9
2_t	877.0	878.2	876.0	878.5
2	863.8	864.6	862.4	865.0
3_t	894.3	896.0	894.1	896.1
3	880.0	881.4	879.7	881.1

The predicted values indicate that regardless of triazane's conformation, it will give off about 20 kJ for every gram combusted. This value is low when compared to our studies of boron molecules, which predict specific enthalpies of combustion ranging from about 40 kJ g^{-1} to about 100 kJ g^{-1} [17–20]. For comparison, methane has a specific enthalpy of combustion of 55.7 kJ g^{-1} [21].

Although not directly computed in Ball's [3] paper on tetrazane, the specific enthalpies of combustion can be calculated relatively easily using his predicted enthalpies of formation. These calculations yield values of -18.5, -18.7, -18.5, and -18.6 kJ g^{-1} for the G2, G3, CBS-QB3, and CBS-APNO methods, respectively. These values are slightly more positive than those calculated for triazane. Due to triazane's slightly larger specific enthalpy of combustion, triazane appears to be a better candidate for a HE material than tetrazane. Triazane's usefulness as a HE material will depend on its density and velocity of combustion, both of which can be determined if it is isolated outside of a silver zeolite solution.

Table 10 lists the proton affinities for each of the three conformations. We assumed that protonation would occur at a nitrogen atom in the molecule. This leads to two possible sites of protonation, the terminal nitrogen atom and the central nitrogen atom. In Table 10, protonation at the terminal nitrogen atom is denoted with a subscript "t". For all three conformations, protonation at the central nitrogen atom led to a lower proton affinity; this is due to the induced positive charge being located between two electron rich sources, the lone pairs on the terminal nitrogen atoms. The predicted proton affinities are similar in value to ammonia's proton affinity, which is 851.4 kJ mol^{-1} [22]. All three conformations have higher proton affinities than ammonia indicating that triazane is a stronger base than ammonia is.

In his study on tetrazane, Ball [3] calculated the proton affinities of tetrazane to be about 1094 kJ mol^{-1} for the terminal nitrogen atom, and 1085 kJ mol^{-1} for the interior nitrogen atoms. These values indicate that the base strength of tetrazane is much greater than triazane. This is to be expected because the extra nitrogen atom is capable of donating its lone pair of electrons to help stabilize the positive charge incurred by the nitrogen atom accepting the proton. This has the effect of making the structure more stable and thus requiring more energy to remove the proton.

Conclusion

We have presented various high level *ab initio* calculations on a new potential HE material, triazane. We have predicted the structure of three of its conformations, along with the vibrational frequencies, infrared intensities, enthalpies of formation, enthalpies of combustion, specific enthalpies of combustion, and proton affinities for each of the three conformations. We have also determined the PES for the conformations by rotation about the N_t-N bond. The predicted specific enthalpy of combustion for triazane is about-20 kJ g^{-1}, which is slightly greater than that of tetrazane. The usefulness of triazane will depend on its density and velocity of detonation, both of which can be determined if triazane is successfully isolated.

Acknowledgements R. M. R. expresses appreciation to the Honors Program at Cleveland State University for their continued support.

References

1. Agrawal JP (1998) Prog Energy Comb Sci 24:1–30
2. Politzer P, Lane P, Concha MC (2005) Computational determination of the energetics of boron and aluminum combustion reactions. In: Manaa MR (ed.), Chemistry at extreme conditions. Elsevier, Amsterdam, pp 473–493
3. Ball DW (2001) J Phys Chem A 105:465–470
4. Schmitz E, Ohme R, Kozakiewicz G (1965) Z Anorgan Allge Chem 339:44–51
5. Kim Y, Gilje JW, Seff J (1977) J Am Chem Soc 99:7057–7059
6. Schlegel HB, Skancke A (1993) J Am Chem Soc 115:7465–7471
7. Fujii T, Selvin CP, Sablier M, Iwase K (2002) J Phys Chem A 106:3102–3105
8. Frisch MJ, Trucks GW, Schlegel HB, Scuseria GE, Robb MA, Cheeseman JR, Zakrzewski VG, Montgomery JA, Stratman RE, Burant JC, Dapprich S, Millam JM, Daniels AD, Kudin KN, Strain MC, Farkas O, Tomasi J, Barone V, Cossi M, Cammi R, Mennucci B, Pomelli C, Adamo C, Clifford S, Ochterski J, Petersson GA, Ayala PY, Cui Q, Morokuma K, Malick DK, Rabuck AD, Raghavachari K, Foresman JB, Cioslowski J, Ortiz JV, Baboul AG, Stefanov BB, Liu C, Liashenko A, Piskorz P, Komaromi, I, Gomperts R, Martin RL, Fox DJ, Keith T, Al-Laham MA, Peng CY, Nanayakkara A, Gonzalez C, Challacombe M, Gill PMW, Johnson BG, Chen W, Wong MW, Andres JL, Gonzales C, Head-Gordon M, Replogle ES, Pople JA (1998) Gaussian 98. Gaussian Inc, Pittsburgh PA
9. Frisch MJ, Trucks GW, Schlegel HB, Scuseria GE, Robb MA, Cheeseman JR, Montgomery Jr JA, Vreven T, Kudin KN, Burant JC, Millam JM, Iyengar SS, Tomasi J, Barone V, Mennucci B, Cossi M, Scalmani G, Rega N, Petersson GA, Nakatsuji H, Hada M, Ehara M, Toyota K, Fukuda R, Hasegawa J, Ishida M, Nakajima T, Honda Y, Kitao O, Nakai H, Klene M, Li X, Knox JE, Hratchian HP, Cross JB, Bakken V, Adamo C, Jaramillo J, Gomperts R, Stratmann RE, Yazyev O, Austin AJ, Cammi R, Pomelli C, Ochterski JW, Ayala PY, Morokuma K, Voth GA, Salvador P, Dannenberg JJ, Zakrzewski VG, Dapprich S, Daniels AD, Strain MC, Farkas O, Malick DK, Rabuck AD, Raghavachari K, Foresman JB, Ortiz JV, Cui Q, Baboul AG, Clifford S, Cioslowski J, Stefanov BB, Liu G, Liashenko A, Piskorz P, Komaromi I, Martin RL, Fox DJ, Keith T, Al-Laham MA, Peng CY, Nanayakkara A, Challacombe M, Gill PMW, Johnson B, Chen W, Wong MW, Gonzalez C, Pople JA, (2004) Gaussian 03. Gaussian Inc, Wallingford CT

10. Dennington II R, Keith T, Millam J, Eppinnett K, Hovell WL, Gilliland R (2003) GaussView, Version 2.1. Semichem Inc, Shawnee Mission, KS
11. Dennington II R, Keith T, Millam J, Eppinnett K, Hovell WL, Gilliland R (2003) GaussView, Version 3.09. Semichem Inc, Shawnee Mission, KS
12. Curtiss LA, Raghavachari K, Trucks GW, Pople JA (1991) J Chem Phys 94:7221–7230
13. Curtiss LA, Raghavachari K, Redfern PC, Rassolov V, Pople JA (1998) J Chem Phys 109:7764–7776
14. Ochterski JW, Petersson GA, Montgomery Jr JA (1996) J Chem Phys 104:2598–2619
15. Gorelsky SI (2006) SWizard program, version 4.1. http://www.sgchem.net
16. NIST Chemistry Webbook, available at http://webbook.nist.gov/chemistry/. Accessed May 12, 2007
17. Richard RM, Ball DW (2006) J Mol Struct-THEOCHEM 776:89–96
18. Richard RM, Ball DW (2007) J Mol Struct -THEOCHEM 806:113–120
19. Richard RM, Ball DW (2007) J Mol Struct-THEOCHEM 806:165170
20. Richard RM, Ball DW (2007) J Mol Struct -THEOCHEM 814:91–98
21. Lide DR (2001) CRC handbook of chemistry and physics, 82nd edn. CRC Press, Boca Raton, FL, p 5–89
22. Szulejko JE, McMahon TB (1993) J Am Chem Soc 115:7839–7848